The Journal of Immunology

RESEARCH ARTICLE | SEPTEMBER 15 2022

Toward Understanding How Staphylococcal Protein A Inhibits IgG-Mediated Phagocytosis

Ana Rita Cruz; ... et. al

J Immunol (2022) 209 (6): 1146–1155.
https://doi.org/10.4049/jimmunol.2200080

Toward Understanding How Staphylococcal Protein A Inhibits IgG-Mediated Phagocytosis

Ana Rita Cruz,* Arthur E. H. Bentlage,† Robin Blonk,* Carla J. C. de Haas,* Piet C. Aerts,* Lisette M. Scheepmaker,* Inge G. Bouwmeester,* Anja Lux,‡ Jos A. G. van Strijp,* Falk Nimmerjahn,‡ Kok P. M. van Kessel,* Gestur Vidarsson,† and Suzan H. M. Rooijakkers*

IgG molecules are crucial for the human immune response against bacterial infections. IgGs can trigger phagocytosis by innate immune cells, like neutrophils. To do so, IgGs should bind to the bacterial surface via their variable Fab regions and interact with Fcγ receptors and complement C1 via the constant Fc domain. C1 binding to IgG-labeled bacteria activates the complement cascade, which results in bacterial decoration with C3-derived molecules that are recognized by complement receptors on neutrophils. Next to FcγRs and complement receptors on the membrane, neutrophils also express the intracellular neonatal Fc receptor (FcRn). We previously reported that staphylococcal protein A (SpA), a key immune-evasion protein of *Staphylococcus aureus*, potently blocks IgG-mediated complement activation and killing of *S. aureus* by interfering with IgG hexamer formation. SpA is also known to block IgG-mediated phagocytosis in absence of complement, but the mechanism behind it remains unclear. In this study, we demonstrate that SpA blocks IgG-mediated phagocytosis and killing of *S. aureus* and that it inhibits the interaction of IgGs with FcγRs (FcγRIIa and FcγRIIIb, but not FcγRI) and FcRn. Furthermore, our data show that multiple SpA domains are needed to effectively block IgG1-mediated phagocytosis. This provides a rationale for the fact that SpA from *S. aureus* contains four to five repeats. Taken together, our study elucidates the molecular mechanism by which SpA blocks IgG-mediated phagocytosis and supports the idea that in addition to FcγRs, the intracellular FcRn is also prevented from binding IgG by SpA. ***The Journal of Immunology*****, 2022, 209: 1146–1155.**

Immunoglobulin Abs play a key role in the host immune response against bacteria. IgGs consist of two functional domains: the Fab and the Fc. Via their variable Fab domain, Abs can directly neutralize the function of bacterial virulence factors. Moreover, when Abs bind to the bacterial surface via their Fab domain, their constant Fc domain can trigger bacterial clearance by interacting with the innate immune system (1). IgG-Fcs have two important effector functions. Although they can directly bind to Fcγ receptors expressed on the surface of innate immune cells, they can also bind complement C1 via clustered IgGs and activate the classical complement pathway. The activation of the complement cascade results in bacterial decoration with C3-derived opsonins, which are, in turn, recognized by complement receptors on innate immune cells, like neutrophils. Both pathways ultimately trigger phagocytosis and killing of the invading bacteria.

FcγRs are membrane glycoproteins and divided into six classes: FcγRI (CD64), FcγRIIa (CD32a), FcγRIIb (CD32b), FcγRIIc (CD32c), FcγRIIIa (CD16a), and FcγRIIIb (CD16b). FcγRI is the only high-affinity receptor, as it can bind to monomeric IgGs, whereas the other receptors mainly bind to aggregated IgGs. The low-affinity receptors have polymorphic variants. Besides the classical extracellular Fc receptors, IgG-Fcs are also recognized by the intracellular neonatal Fc receptor (FcRn) (2) (Fig. 1A). FcRn is found on different cell types, including epithelial cells, endothelial cells, and placental syncytiotrophoblasts. FcRn is mainly known for its role in transferring IgG from the mother to the fetus (3) and in the regulation of IgG half-life (4, 5). More recently, FcRn was also found to be expressed in monocytes, macrophages, dendritic cells (6), and neutrophils (2) and shown to be involved in phagocytosis of IgG-coated pneumococci (2). The binding sites of FcγRs and FcRn on IgG are different (Fig. 1B): whereas FcγRs bind with a 1:1 stoichiometry to the lower hinge and CH2 domain of IgG (7), FcRn binds the CH2–CH3 interface of IgG with a 2:1 stoichiometry (8–10). Another difference is that FcRn-IgG binding only occurs at acidic pH (<6.5) (11).

Interestingly, the Fc fragment of IgGs is not only recognized by host immune effector proteins, but also by bacterial immune-evasion molecules (12), like staphylococcal protein A (SpA). SpA is a key immune-evasion factor of *Staphylococcus aureus*, a prominent human pathogen that spreads in health care facilities and in the community, causing multiple diseases (13).

SpA is mainly anchored to the bacterial cell wall, although it is also found in the extracellular milieu (14, 15). SpA is composed of five

*Department of Medical Microbiology, University Medical Center Utrecht, Utrecht University, Utrecht, the Netherlands; †Department of Experimental Immunohematology, Sanquin Research and Landsteiner Laboratory, Academic Medical Center, University of Amsterdam, Amsterdam, the Netherlands; and ‡Division of Genetics, Department of Biology, Friedrich-Alexander-University of Erlangen-Nürnberg, Erlangen, Germany

Received for publication January 25, 2022. Accepted for publication July 13, 2022.

ORCIDs: 0000-0002-3870-7576 (A.R.C.); 0000-0002-7924-554X (A.E.H.B.); 0000-0002-5203-2448 (R.B.); 0000-0003-3819-3349 (L.M.S.); 0000-0002-2858-6993 (I.G.B.); 0000-0001-9475-2147 (A.L.); 0000-0001-6253-0830 (J.A.G.v.S.); 0000-0003-1268-5484 (K.P.M.v.K.); 0000-0001-5621-003X (G.V.); 0000-0003-4102-0377 (S.H.M.R.).

This work was supported by the European Union's Horizon 2020 research programs H2020–Marie Skłodowska-Curie Actions–Innovative Training Networks Grant 675106 to J.A.G.v.S., European Research Council Starting Grant 639209 to S.H.M.R., and Deutsche Forschungsgemeinschaft CRC1181-A07 to F.N. and FOR 2886 to F.N. and A.L.

Address correspondence and reprint requests to Dr. Suzan H. M. Rooijakkers, University Medical Center Utrecht, Medical Microbiology, Heidelberglaan 100, Utrecht 3584 CX, the Netherlands. E-mail address: s.h.m.rooijakkers@umcutrecht.nl

The online version of this article contains supplemental material.

Abbreviations used in this article: CHO, Chinese hamster ovary; FcRn, neonatal Fc receptor; FLIPr-like, formyl peptide receptor-like 1 inhibitor; hFcγR, human FcγR; HI-NHS, heat-inactivated normal human serum; HSA, human serum albumin; mAm, mAmetrine; PBS-T, PBS 0.05% v/v with Tween-20; PBS-TH, PBS 0.05% v/v with Tween-20 and 0.5% human serum albumin; RPMI-H, RPMI-1640 plus 0.05% human serum albumin; SpA, staphylococcal protein A; SpA-B, B domain of staphylococcal protein A; SpA-5xB, repeating five B-domain staphylococcal protein A; SPR, surface plasmon resonance; WT, wild-type; WTA, wall teichoic acid.

highly homologous three-helix-bundle domains (named A to E), each of which can bind the CH2–CH3 interface of IgG (Figs. 1B, 2A), via helices I and II (16). Moreover, SpA domains also bind the Fab region of most VH3-type family of Abs, via helices II and III (17). Of note, the Fc domain recognition properties of SpA are subclass and allotype specific. SpA binds IgG1, IgG2, and IgG4 subclasses, but not to the majority of IgG3 allotypes (18, 19). This is due to an amino acid substitution in position 435, where a histidine in IgG1, IgG2, and IgG4 becomes an arginine in most of IgG3 allotypes (20, 21). Therefore, the effector functions of IgG3 remain unaffected by the presence of SpA (22).

We and others showed that SpA protects *S. aureus* from phagocytic killing by binding the IgG-Fc fragment (22–24). In our previous study, we unveiled how SpA blocks IgG-mediated complement activation and subsequent killing of *S. aureus* (22). We showed that SpA binds competitively to the Fc–Fc interaction interface on IgG monomers, which effectively prevents IgGs from forming IgG hexamers (22). IgG hexamerization on antigenic surfaces is important for efficient binding of C1 and subsequent activation of the complement system (25).

However, SpA was also reported to prevent IgG-dependent phagocytic killing in the absence of complement (24). To date, the precise mechanism by which SpA blocks FcγR-mediated phagocytosis remains elusive. SpA is known to reduce binding of Ag-complexed and heat-aggregated IgG to Fc receptor-bearing cells (26). However, soluble FcγRI and FcγRIIa were shown not to compete with SpA for binding to soluble IgG (27). In this study, we investigate how SpA interferes with FcR-mediated phagocytosis of *S. aureus*.

Materials and Methods

Production of human mAbs

The human anti-DNP and anti–wall teichoic acid (WTA) GlcNAc-β-4497 monoclonal IgG1 and IgG3 (IGHG3*01) were produced recombinantly in human Expi293F cells (Life Technologies, Carlsbad, CA), as described before (22). The VH and VL sequences of the anti-DNP (DNP-G2a2) (28) and anti-WTA GlcNAc-β-4497 (patent WO/2014/193722) (29) were derived from previously reported Abs. The point mutations H435R and Y436F were introduced in the H chain expression vectors by PCR using reverse primers carrying the mutations. The changes made in the VH region of anti-WTA GlcNAc-β-4497 IgG1 to convert it into a functional VH3 chain were based on a previous study (30). The human anti–TNF-α IgG1 mAb was expressed in the HEK-293F FreeStyle cell line expression system (Life Technologies) with cotransfection of vectors encoding p21, p27, and pSVLT genes to increase protein production (31). The VH and VL sequences of the anti–TNF-α (U.S. patent 6090382A) were also derived from a previously published Ab. Anti–TNF-α IgG1 was purified on Protein A HiTrap HP columns (GE Healthcare Life Sciences, Little Chalfont, U.K.) using AKTA Prime Plus (GE Healthcare Life Sciences) and dialyzed overnight against PBS.

Cloning, expression, and purification of staphylococcal proteins

SpA constructs were cloned, expressed, and purified as reported previously (22). The wild-type (WT) B domain of SpA (SpA-B), SpA-B lacking Fc-binding properties (SpA-B^{KK}; Q9K and Q10K mutations), and SpA-B lacking Fab-binding properties (SpA-B^{AA}; D36A and D37A mutations) were produced for a previous study (22), whereas the five-domain SpAs (SpA-WT) and the repeating five B-domain SpAs (SpA-5xB) were newly produced, following the same steps described before (22). For the design of SpA-5xB, multiple attempts were made to rearrange its nucleotide sequence to make the synthesis as the gBlock (Integrated DNA Technologies) possible. Besides the in-house–produced SpA-WT, for some of the experiments, we used a five-domain SpA (also named SpA-WT) that is commercially available (PRO-1925; ProSpec). The recombinant protein formyl peptide receptor-like 1 inhibitor (FLIPr-like) was expressed and purified as described before (32).

Bacterial strains and culture conditions

The fluorescent reporter mAmetrine (mAm) was used to label *S. aureus* Newman Δ*spa*/*sbi* and Newman WT, as described before (33). Briefly, bacteria were transformed with a pCM29 plasmid that constitutively and robustly expresses a codon-optimized mAm protein (https://www.ncbi.nlm.nih.gov/nuccore/KX759016) (34) from the sarAP1 promoter (35). For generation of p*spa*-complemented Newman Δ*spa*/*sbi*, the *spa* gene and its promoter were first PCR amplified from genomic DNA of *S. aureus* Newman WT. The PCR products were cloned into the pCM29 vector via Gibson assembly and *Escherichia coli* DC10b transformed with pCM29-*spa* by heat shock. Subsequently, the plasmid was isolated, and competent *S. aureus* Newman Δ*spa*/*sbi* were transformed with the plasmid through electroporation using the Bio-Rad Gene Pulser Xcell Electroporation System (200 Ω, 25 μF, and 2.5 kV). After recovery, bacteria were plated on Todd Hewitt agar supplemented with 5 μg/ml chloramphenicol to select plasmid-complemented colonies. Bacteria were grown overnight in Todd Hewitt broth plus 10 μg/ml chloramphenicol, diluted to an OD_{600} of 0.05 in fresh Todd Hewitt broth plus chloramphenicol, and cultured until midlog phase (OD_{600} = 0.5). The mAm-expressing strains Newman Δ*spa*/*sbi* and Newman WT were washed and resuspended in RPMI-1640 plus 0.05% human serum albumin (HSA) (RPMI-H medium) and stored until use at −20°C. The Newman Δ*spa*/*sbi* + p*spa* strain was FITC-labeled before storage. Briefly, midlog phase bacteria were washed with PBS and resuspended in 0.5 mg/ml FITC (Sigma-Aldrich) in PBS for 1 h on ice, washed twice in PBS, resuspended in RPMI-H medium, and stored until use at −20°C.

Phagocytosis of S. aureus *by neutrophils*

Human neutrophils were purified from blood of healthy donors by the Ficoll/Histopaque density gradient method (36). To study the inhibitory effect of SpA on phagocytosis, we used a recently described phagocytosis assay (33), with some adaptations. Fluorescently labeled (mAm-expressing) Newman Δ*spa*/*sbi* (7.5×10^5 CFU) was first incubated with human monoclonal anti-WTA IgG1 for 15 min at 37°C with shaking (± 700 rpm) in a round-bottom microplate. After, bacteria were washed with RPMI-H by centrifugation (3600 rpm, 7 min) and incubated in absence or presence of SpA-B, SpA-WT, SpA-5xB, or FLIPr-like for 15 min at 37°C with shaking. Finally, bacteria were mixed with neutrophils for another 15 min at 37°C with shaking, at a 10:1 bacteria/neutrophil ratio. Alternatively, bacteria were simultaneously incubated with human monoclonal anti-WTA IgG1, IgG3, IgG1(VH3)-H435R/Y436F, heat-inactivated normal human serum (HI-NHS) with buffer, SpA constructs, or FLIPr-like in RPMI-H medium for 15 min at 37°C with shaking. Bacteria were then incubated with freshly isolated neutrophils for another 15 min at 37°C with shaking. To evaluate the inhibitory effect of cell-attached SpA on phagocytosis, 7.5×10^5 CFU of fluorescently labeled Newman Δ*spa*/*sbi*, Newman WT, or Newman Δ*spa*/*sbi* + p*spa* were incubated with anti-WTA IgG1, IgG3, or HI-NHS in RPMI-H. After 15 min at 37°C with shaking, IgG-opsonized bacteria were incubated with 7.5×10^4 neutrophils for another 15 min at 37°C with shaking. All samples were fixed with 1% paraformaldehyde in RPMI-H. The binding/internalization of mAm bacteria to the neutrophils was detected using flow cytometry (BD FACSVerse), and data were analyzed based on forward/side scatter gating of neutrophils using FlowJo software.

Killing of S. aureus *by neutrophils*

mAm-expressing Newman Δ*spa*/*sbi* were freshly grown to midlog phase, washed with PBS, and resuspended in HBSS plus 0.1% HSA medium. A total of 8.5×10^5 CFU Newman Δ*spa*/*sbi* was incubated with 4-fold titration of anti-WTA IgG1 or IgG3 in the absence or presence of 200 nM SpA-B or SpA-WT in HBSS plus 0.1% HSA. After 30 min at 37°C, bacteria were incubated with neutrophils for 90 min under 5% CO_2 at 37°C, at a 1:1 bacteria/neutrophil ratio. Subsequently, neutrophils were lysed with cold 0.3% w/v saponin in water for up to 15 min on ice. Samples were serially diluted in PBS and plated in duplicate onto tryptic soy agar plates, which were incubated overnight at 37°C. Viable bacteria were quantified by CFU enumeration.

ELISAs

MaxiSorp plates (Nunc) were coated with 3 μg/ml SpA-B, SpA-B^{KK}, SpA-B^{AA} in 0.1 M sodium carbonate at 4°C overnight. After three washes with PBS 0.05% v/v with Tween-20 (PBS-T; pH 7), the wells were blocked with 4% BSA in PBS-T for 1 h at 37°C. The following incubations were performed for 1 h at 37°C followed by three washes with PBS-T. A total of 1 μg/ml of anti-WTA IgG1, anti-WTA IgG3, or IgG1(VH3)-H435R/Y436F was diluted in 1% BSA in PBS-T and added to the wells. Bound Abs were detected with HRP-conjugated goat F(ab′)$_2$ anti-human κ (SouthernBiotech) in 1% BSA in PBS-T and tetramethylbenzidine as substrate. The reaction was stopped with 1 N sulfuric acid, and absorbance was measured at 450 nm in the iMark Microplate Absorbance Reader (Bio-Rad Laboratories).

SpA expression and Ab binding on S. aureus *Newman strains*

To detect cell-attached SpA, 7.5×10^5 CFU of fluorescently labeled *S. aureus* Newman strains (Δ*spa*/*sbi*, WT, and Δ*spa*/*sbi* + p*spa*) were

incubated in a round-bottom microplate with 1 μg/ml biotin-conjugated chicken anti–Protein A (Immunology Consultants Laboratory) in RPMI-H for 30 min at 4°C under shaking conditions (± 700 rpm), washed by centrifugation with RPMI-H (3600 rpm, 7 min), and incubated with 2 μg/ml Alexa Fluor 647–conjugated streptavidin (Jackson ImmunoResearch Laboratories) in RPMI-H for another 30 min at 4°C under shaking conditions. To measure Ab binding to the same strains, bacteria (7.5×10^5 CFU) were incubated with 3-fold serial dilutions of anti-DNP IgG1 or IgG3, anti-WTA IgG1, or IgG3 in RPMI-H (starting from 10 nM IgG) for 30 min at 4°C, with shaking. Subsequently, bacteria were washed by centrifugation with RPMI-H (3600 rpm, 7 min) and incubated with 0.5 μg/ml Alexa Fluor 647–conjugated goat $F(ab')_2$ anti-human κ (Southern Biotech) in RPMI-H for 30 min at 4°C under shaking conditions. After an additional wash with RPMI-H, all samples were fixed with 1% paraformaldehyde in RPMI-H. SpA expression and Ab binding on *S. aureus* Newman strains were detected using flow cytometry (BD FACSVerse), and data were analyzed using FlowJo software.

Surface plasmon resonance measurements

Affinity measurements of soluble IgG to FcγRs and FcRn were performed with the IBIS-MX96 biosensor system as described previously (37). In short, C-terminally site-specifically BirA-biotinylated human FcγRs (hFcγRs) [FcγRIIa H131, FcγRIIa R131, FcγRIIb, FcγRIIIa F158, FcγRIIIa V158, FcRn (10374-H27H1-B, 10374-H27H-B, 10259-H27H-B, 10389-H27H-B, 10389-H27H1-B, and CT071-H27H-B, respectively; Sino Biological), FcγRIIIb NA1, and FcγRIIIb NA2 (produced at the laboratory of Sanquin)] were spotted onto a SensEye G-Streptavidin sensor (Senss, Enschede, the Netherlands) using a continuous flow micro spotter (Wasatch Microfluidics, Salt Lake City, UT) in running buffer (PBS 0.0075% Tween-80; AMRESCO; pH 7.4). The receptors were added at the following concentrations: 10 nM of FcγRIIa H131, FcγRIIa R131, and FcγRIIb; 30 nM of FcγRIIIa 158F, FcγRIIIb NA1, and FcγRIIIb NA2; and 100 nM of FcγRIIIa 158V. For IgG-FcγRI binding measurements, 30 nM of biotinylated mouse IgG1 anti-His was first spotted on the sensor, followed by 50 nM of His-tagged FcγRI (10256-H27H; Sino Biological). A total of 200 nM anti–TNF-α IgG1 was then injected in combination with 1 μM or 200 nM SpA-B, SpA-WT, or SpA-5xB or running buffer. For IgG-FcRn binding measurements, the running buffer was at a pH of 6. Regeneration after each sample was carried out with 10 mM Gly-HCl (pH 2.4).

Binding assays with hFcγR-expressing Chinese hamster ovary cell lines

Chinese hamster ovary (CHO) cells expressing hFcγRI, FcγRIIa H131, FcγRIIa R131, FcγRIIIb NA1, or FcγRIIIb NA2 were generated at a University of Erlangen-Nürnberg laboratory (38). Untransfected CHO cells were maintained in RPMI medium supplemented with 10% FCS, 2 mM glutamine, 1 mM sodium pyruvate, 0.1 mg/ml penicillin/streptomycin, and 0.1 mM nonessential amino acids at 37%, 5% CO_2, whereas for the CHO cell lines stably transfected with hFcγRs, 0.05 mg/ml G418 was also added to the supplemented RPMI medium. Cells were collected by brief trypsinization, washed, and resuspended in RPMI-H. Viability was >95% as assessed with trypan blue. Specific FcγR expression by the CHO cells was confirmed by using Abs raised against each of the FcγR classes. CHO cells (7.5×10^4 cells) were incubated with FITC-labeled anti-human CD64 IgG1 clone 10.1 (Fitzgerald), PE-labeled anti-human CD32 IgG2b clone 7.3 (Fitzgerald), or PE-labeled anti-human IgG1 clone 3G8 CD16 (BD Biosciences) in RPMI-H for 30 min at 4°C with shaking (± 700 rpm) in a round-bottom microplate, and after washing by centrifugation with RPMI-H ($125 \times g$, 7 min). For the bacteria binding assays, mAm-expressing Newman Δ*spa*/*sbi* (7.5×10^5 CFU or 2.25×10^6 CFU) was first labeled with anti-WTA IgG1 or buffer control for 30 min at 4°C with shaking (± 700 rpm) in a round-bottom microplate in RPMI-H. Bacteria were washed by centrifugation with RPMI-H (3600 rpm, 7 min) and, after mixing with buffer, SpA-B, SpA-WT, SpA-5xB, or FLIPr-like in RPMI-H for 30 min at 37°C with shaking. Finally, CHO cells (7.5×10^4 cells) were added to the mixture (10:1 bacteria/cells ratio for FcγRI-, FcγRIIa H131-, and FcγRIIa R131-expressing CHO cells and 30:1 bacteria/cells ratio for FcγRIIIb NA1- and FcγRIIIb NA2-expressing CHO cells) for another 30 min at 37°C with shaking. The reaction was stopped and fixed by addition of 1% paraformaldehyde in RPMI-H. FcγR expression and binding of mAm bacteria to the CHO cells were measured by flow cytometry (BD FACSVerse), and data were analyzed based on forward light scatter/side scatter gating of CHO cells using FlowJo software.

FcRn receptor–coated bead assays

Streptavidin beads (Dynabeads M-270; Invitrogen) were washed in PBS 0.05% v/v with Tween-20 and 0.5% HSA (PBS-TH) and incubated (diluted 100 times) with 1 μg/ml C-terminally site-specifically BirA-biotinylated hFcRn (FCM-H82W7; ACROBiosystems) in PBS-TH for 30 min at 4°C with shaking. FcRn-labeled beads were then washed twice with PBS-TH and resuspended in PBS-TH at a pH of 6. For binding of bacteria-bound IgG to FcRn-coated beads, mAm-expressing Newman Δ*spa*/*sbi* (6×10^5 CFU) was first incubated with anti-WTA IgG1 in RPMI-H for 30 min at 4°C with shaking (± 700 rpm). From this step, all incubations and washes were performed using PBS-TH (pH 6). After a single wash by centrifugation (3600 rpm, 7 min), IgG1-labeled bacteria were incubated in absence or presence of SpA-B, SpA-WT, or SpA-5xB for 30 min at 37°C with shaking. FcRn-coated beads were then mixed with the bacteria for 30 min at 37°C with shaking. For each condition, 0.5 μl of FcRn-coated beads were used (~3×10^5 beads/condition). After two washes, the beads were incubated with 1 μg/ml Alexa Fluor 647–conjugated goat $F(ab')_2$ anti-human κ (2062-31; SouthernBiotech) for 30 min at 4°C with shaking. For binding of soluble IgG to FcRn-coated beads, anti-DNP IgG1 was first incubated in absence or presence of recombinant SpA-B, SpA-WT, SpA-5xB, or FLIPr-like in a round-bottom microplate at 4°C with shaking. After 30 min of incubation, IgG1 plus Buffer/SpA/FLIPr-like was mixed with FcRn-labeled beads for another 30 min at 37°C with shaking. After two washes, the beads were incubated with 1 μg/ml Alexa Fluor 647–conjugated goat $F(ab')_2$ anti-human κ (2062-31; SouthernBiotech) for 30 min at 4°C with shaking. Finally, the beads were washed twice and then fixed with 1% paraformaldehyde in PBS-TH. Binding of bacteria-bound IgG and soluble IgG to the beads was detected using flow cytometry (BD FACSVerse), and data were analyzed based on a single bead population using FlowJo software.

Ethical statement

Human serum and blood were obtained from healthy donors after informed consent was obtained from all subjects, in accordance with the Declaration of Helsinki. Approval from the Medical Ethics Committee of the University Medical Center Utrecht was obtained (METC protocol 07-125/C, approved March 1, 2010).

Statistical analysis

Statistical analysis was performed with Prism v.8.3 software (GraphPad) using one-way ANOVA, as indicated in the figure legends. At least three experimental replicates were performed to allow statistical analysis.

Results

Soluble SpA requires multiple domains to effectively block IgG1-mediated phagocytosis and killing of S. aureus

To investigate how SpA blocks IgG-mediated phagocytosis (Fig. 1), we first studied whether different forms of soluble SpA affect phagocytosis of *S. aureus* by human neutrophils. To exclusively determine the effect of soluble SpA in this assay, we used an isogenic mutant of Newman *S. aureus* strain lacking both SpA and the second Ig-binding protein of *S. aureus*, Sbi (39) (Newman Δ*spa*/*sbi*). Newman Δ*spa*/*sbi* was first incubated with a human IgG1 mAb that targets WTA (anti-WTA IgG1). WTA is a highly abundant surface glycopolymer anchored to the peptidoglycan layer of *S. aureus* (40). After a wash to remove unbound IgGs, IgG1-labeled bacteria were incubated with different recombinant SpA constructs: SpA-WT composed of five IgG-binding domains, a single SpA-B, and an SpA variant composed of five repeating B domains (SpA-5xB) (Fig. 2A). As a positive control, we used the homolog of FLIPr-like, a staphylococcal FcγR inhibitor (that directly binds and blocks FcγRs) that has been shown to decrease phagocytosis of Ab-coated bacteria (41). Although SpA-WT and SpA-5xB potently reduced phagocytosis mediated by IgG1, the single SpA-B domain showed a minimal effect on phagocytosis (Fig. 2B, Supplemental Fig. 1A).

To understand whether the SpA constructs could also inhibit phagocytosis when in presence of soluble IgGs, we also assessed phagocytosis when bacteria, IgGs, and SpA were incubated at the same step. In this setup in which SpA can interact with both target-bound and soluble Abs, we observed that multidomain SpA can still inhibit IgG1-mediated phagocytosis, although the inhibitory effect was slightly weaker (Fig. 2C, Supplemental Fig. 1B).

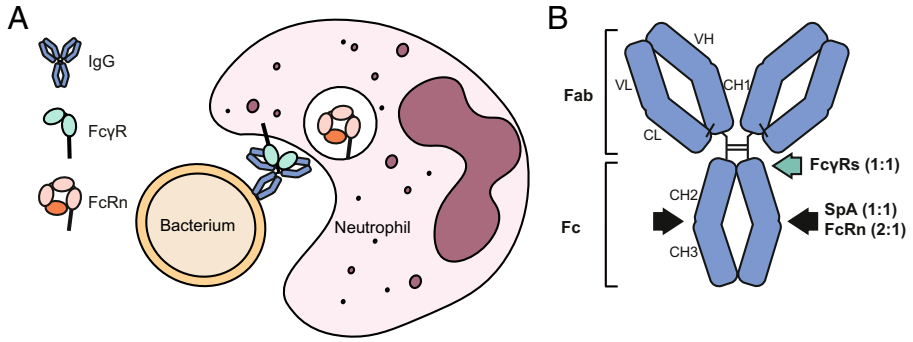

FIGURE 1. Neutrophils express FcγRs and FcRn that recognize IgG-Fcs in structurally distant sites. (**A**) Schematic representation of an IgG-labeled bacterium being phagocytized by a neutrophil, showing binding of extracellular FcγRs to IgGs and FcRn inside granular structures. (**B**) Schematic illustration of IgG indicating the binding regions of SpA, FcγRs, and FcRn. FcγRs bind to the lower hinge and CH2 domain of IgG with a 1:1 stoichiometry, whereas SpA and FcRn bind to the CH2–CH3 interface with a 1:1 and 2:1 stoichiometry, respectively.

When, instead of anti-WTA IgG1 Abs, we used a IgG3 allotype that does not bind SpA, none of the SpA constructs affected phagocytosis (Fig. 2D), suggesting that SpA interferes with IgG-mediated phagocytosis by binding to the Fc region of IgGs. To confirm that SpA blocks IgG-mediated phagocytosis by specific binding to the IgG-Fc region and not to the IgG-Fab domain, we modified the anti-WTA IgG1 molecule in such a way that it only interacts with SpA via Fab. Although anti-WTA Ab clone 4497 used in these assays belongs to VH3-type family (42), it does not bind SpA via its Fab region (22). Therefore, we modified the VH region of anti-WTA IgG1 to gain SpA-Fab binding (IgG1 [VH3]). In addition, we abrogated binding of SpA to Fc, by introducing mutations at H435R and Y436F in the IgG-Fc region (20). The SpA binding properties of anti-WTA IgG1(VH3)-H435R/Y436F, as well as anti-WTA IgG1 and IgG3, were verified by comparing their binding to the WT SpA-B with two SpA-B variants that cannot interact with Fc (SpA-B^{KK}) or Fab (SpA-B^{AA}) domains of IgG (Supplemental Fig. 1C, 1D). We showed that anti-WTA IgG1(VH3)-H435R/Y436F was equally effective in mediating phagocytosis as its WT variant (compare Fig. 2C with Supplemental Fig. 1E). However, in contrast to the WT Ab, SpA did not significantly reduce phagocytosis by IgG1 (VH3)-H435R/Y436F (Supplemental Fig. 1E). This demonstrates that soluble SpA blocks IgG-mediated phagocytosis by specific binding to the IgG-Fc region.

Next, we evaluated whether inhibition of IgG-mediated phagocytosis by SpA results in less phagocytic killing of *S. aureus* by human neutrophils. Upon engulfment, neutrophils can kill bacteria intracellularly by exposing them to antimicrobial peptides, enzymes, and reactive oxygen species (43). Although anti-WTA IgG1 Abs alone induced killing of *S. aureus*, the presence of SpA-WT blocked killing (Fig. 2E). In line with the phagocytosis data, we observed that a single SpA-B domain cannot block IgG1-mediated killing (Fig. 2E). As expected, the presence of SpA proteins did not affect IgG3-mediated killing of *S. aureus* (Fig. 2F).

Altogether, these data suggest that soluble SpA blocks phagocytosis and killing of *S. aureus* by binding to the Fc region of IgG. Furthermore, we find that multiple SpA domains are required to potently block IgG-mediated phagocytosis.

Surface-bound SpA blocks IgG-mediated phagocytosis of S. aureus

Next, we assessed whether surface-attached SpA also reduces IgG-mediated phagocytosis. To do so, we compared phagocytosis of WT *S. aureus* strain Newman with Newman Δ*spa*/*sbi*. In addition, we complemented Newman Δ*spa*/*sbi* with SpA by overexpressing the *spa* gene from a plasmid (Newman Δ*spa*/*sbi* + p*spa*). SpA overexpression on the *S. aureus* Newman Δ*spa*/*sbi* + p*spa* surface was validated by anti-SpA IgY Abs and flow cytometry (>3-fold expression than in the WT strain; Fig. 3A). Moreover, SpA functionality on the bacterial surface was confirmed by studying that an IgG1 isotype control (anti–2,4-DNP Ab) can bind cell-surface SpA-expressing strains (Newman WT and Newman Δ*spa*/*sbi* + p*spa*), but not Newman Δ*spa*/*sbi* (Supplemental Fig. 2A). As anticipated, anti-DNP IgG3 (IGHG3*01) Abs did not bind any of the Newman strains (Supplemental Fig. 2B). Next, we compared phagocytosis of these three strains in the presence of monoclonal IgGs directed against WTA. After IgG1 and IgG3 were confirmed to similarly bind to the three Newman strains (Supplemental Fig. 2C, 2D), we showed that IgG1-mediated phagocytosis was lower for the cell-surface SpA-expressing strains than for the knockout strain (Fig. 3B). Notably, the inhibitory effect of SpA on phagocytosis was even more prominent when SpA was overexpressed (Fig. 3B). All three bacterial strains were efficiently phagocytized when labeled with anti-WTA IgG3 Abs (Fig. 3C). Overall, these data suggest that, similar to soluble SpA, cell-surface SpA also reduces IgG-mediated phagocytosis of *S. aureus* by binding to the IgG-Fc region.

Soluble, multidomain SpA affects binding of bacterium-bound IgG1 to FcγRIIa and FcγRIIIb, but not to FcγRI

Because FcγRs are generally believed to be the main drivers of IgG-mediated phagocytosis, we studied whether SpA could interfere with IgG-FcγRs interactions. Although neutrophils mainly express FcγRIIa and FcγRIIIb on their surface, FcγRI is found at low abundance (44, 45). Thus, we focus on the effect of SpA on IgG binding to these three FcγR classes. We performed binding assays of IgG1-labeled Newman Δ*spa*/*sbi* to membrane-bound FcγRs using CHO cell lines that stably express single hFcγRs (38). These include FcγRI, FcγRIIa, and FcγRIIIb and the respective polymorphic variants (FcγRIIa H131, FcγRIIa R131, FcγRIIIb NA1, and FcγRIIIb NA2). The expression of each FcγR class by the CHO cells was confirmed by use of anti-human CD32, CD64, and CD16 Abs (Supplemental Fig. 3A–C). We observed that the presence of the SpA constructs did not affect binding of IgG1-coated bacteria to hFcγRI-expressing CHO cells (Fig. 4A, Supplemental Fig. 3D). However, the multidomain SpA proteins reduced the binding of IgG1-labeled bacteria to hFcγRIIa-expressing CHO cells (Fig. 4B, 4C, Supplemental Fig. 3E, 3F) and to hFcγRIIIb-expressing CHO cells (Fig. 4D, 4E, Supplemental Fig. 3G, 3H). Curiously, the single B domain also decreased the binding of IgG1-coated bacteria to hFcγRIIIb-expressing CHO cells, although less efficiently than multidomain SpA (Fig. 4D, 4E, Supplemental Fig. 3G, 3H). Of note, we confirmed that IgG1-bound bacteria were unable to bind untransfected CHO cells (Supplemental Fig. 3I, 3J). Taken together, these results show that soluble SpA composed of five domains interferes

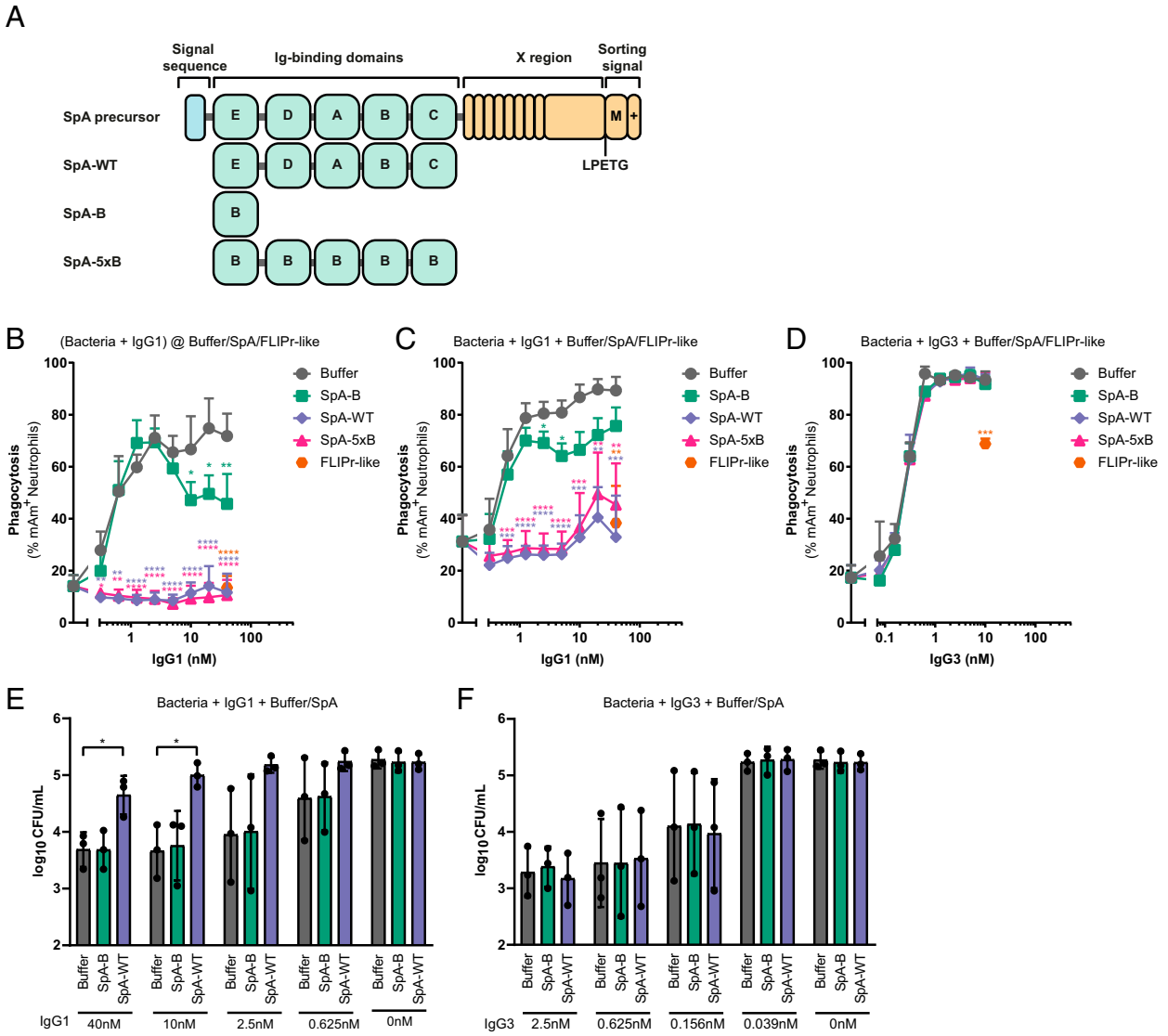

FIGURE 2. Soluble SpA requires multiple domains to effectively block IgG1-mediated phagocytosis and killing of *S. aureus*. (**A**) Schematic representation of SpA precursor and recombinant SpA proteins used in this study. Unprocessed SpA consists of a signal sequence, five Ig-binding domains (E, D, A, B, and C), an X region, and a sorting region. The rSpA proteins used in this study include solely the Ig-binding domains. Although SpA-WT is composed of five different Ig-binding domains, SpA-B contains a single B domain, and SpA-5xB consists of five repeating B domains. (**B**) Phagocytosis of *S. aureus* Newman Δ*spa*/*sbi* after incubation of bacteria with a concentration range of anti-WTA IgG1, followed by buffer (gray) or 200 nM of SpA-B (green), SpA-WT (blue), SpA-5xB (pink), or FLIPr-like (orange), measured by flow cytometry. Bacteria were washed after incubation with IgGs to remove unbound IgG and only after buffer, SpA, or FLIPr-like was added. Phagocytosis of *S. aureus* Newman Δ*spa*/*sbi* after incubation of bacteria with a concentration range of anti-WTA IgG1 (**C**) or IgG3 (**D**), in absence (buffer; gray) or presence of 200 nM soluble SpA-B (green), SpA-WT (blue), SpA-5xB (pink), or FLIPr-like (orange), measured by flow cytometry. Bacteria, IgG and buffer, SpA, or FLIPr-like were incubated at the same step. CFU enumeration of Newman Δ*spa*/*sbi* after incubation with anti-WTA IgG1 (**E**) or IgG3 (**F**) in absence (buffer; gray) or presence of 200 nM SpA-B (green) or SpA-WT (blue), followed by incubation with human neutrophils. Bacteria, IgG and buffer, SpA, or FLIPr-like were incubated at the same step. Data are presented as percentage of mAm^+ neutrophils ± SD of three (B and C) or two (D) independent experiments, or as $\log_{10}$ CFU/ml ± SD of three independent experiments (E and F). Statistical analysis was performed using one-way ANOVA to compare buffer condition with SpA-B, SpA-WT, SpA-5xB, and FLIPr-like conditions and displayed only when significant as $^*p \leq 0.05$, $^{**}p \leq 0.01$, $^{***}p \leq 0.001$, $^{****}p \leq 0.0001$.

with the binding of IgG1-coated bacteria to membrane bound FcγRIIa and FcγRIIIb, but not with FcγRI, and that SpA-B can only interfere with IgG-FcγRIIIb binding.

Soluble, multidomain SpA affects binding of soluble IgG1 to all FcγR classes, except FcγRI

Although our assays with target-bound IgG1 indicate that multidomain SpA blocks FcγRIIa-IgG1 and FcγRIIIb-IgG1 interactions, a previous study showed that SpA does not compete with FcγRIIa to bind soluble IgG1 (27). Although it is more relevant to investigate how SpA competes with FcγR for binding to target-bound IgG than to soluble IgG, we also performed surface plasmon resonance (SPR) experiments to assess the effects of our defined SpA fragments on binding of soluble IgG1 to all FcγR classes and polymorphic variants. FcγRs were coupled to streptavidin biosensors and soluble IgG1 in presence or absence SpA were subsequently injected (Supplemental Fig. 4A). In this setup, we measure binding in a label-free manner, and thus, the strength of the signal is dependent on m.w., which is increased if IgG-SpA complexes bind to FcγRs. Therefore, when compared with IgG1 in absence of SpA (buffer condition), an increase in signal simply means that IgG-SpA complexes are binding to FcγRs. Lower signal indicates that SpA blocks

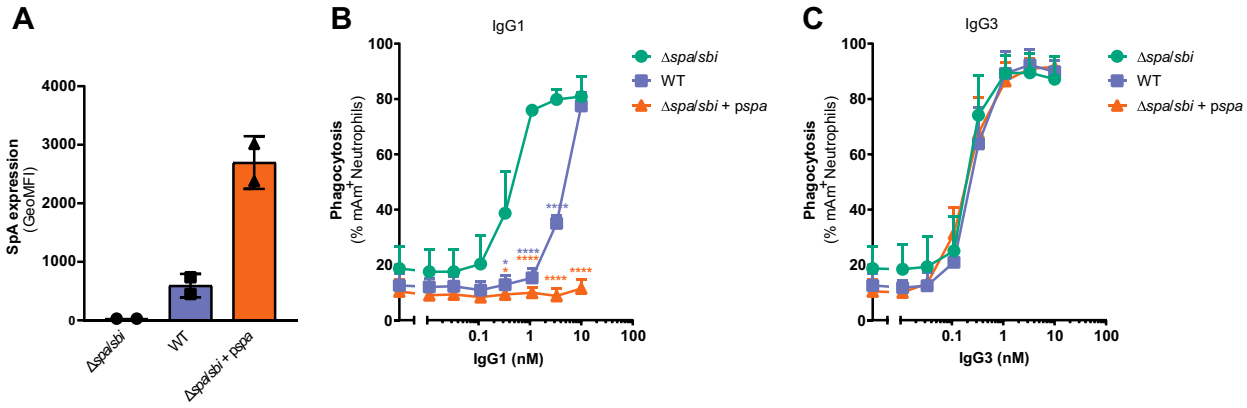

FIGURE 3. Cell-anchored SpA blocks IgG-mediated phagocytosis of *S. aureus* by binding to IgG-Fc domains. (**A**) SpA expression on the surface of Newman Δ*spa/sbi,* Newman WT, and Newman Δ*spa/sbi* + p*spa*, detected with biotinylated-anti-SpA IgY, by flow cytometry. Phagocytosis of *S. aureus* Newman Δ*spa/sbi*, Newman WT, and Newman Δ*spa/sbi* + p*spa* strains after incubation of bacteria with a concentration range of anti-WTA IgG1 (**B**) or IgG3 (**C**), measured by flow cytometry. Data are presented as geometric mean fluorescence intensity (GeoMFI) ± SD of two independent experiments (A) or as percentage of mAm^+ neutrophils or $FITC^+$ neutrophils ± SD of three independent experiments (B and C). (B and C) Statistical analysis was performed using one-way ANOVA to compare Newman Δ*spa/sbi* conditions with Newman WT and Newman Δ*spa/sbi* + p*spa* conditions and displayed only when significant as $*p \leq 0.05$, $****p \leq 0.0001$.

IgG-FcγR interaction, whereas equal signal suggests something in between: perhaps partial blocking. Contrasting with what was previously reported (27), we found that the multidomain SpA proteins reduced the interaction of IgG1 to all FcγRs coated on the chip (the signal is lower than with buffer), except to FcγRI (the signal is higher than with buffer) (Supplemental Fig. 4B). Compared to buffer alone, monovalent SpA-B SPR responses are increased, indicating binding of IgG1-SpA-B complexes with FcγRs (Supplemental Fig. 4B). Altogether, these results show that multidomain SpA can still interfere with binding of soluble IgG1 to low-affinity FcγRs, whereas SpA-B does not.

Soluble SpA inhibits IgG1-FcRn interactions

Besides extracellular FcγRs, neutrophils also express FcRn inside granular structures (2) (Fig. 1A). The presence of FcRn in neutrophils was shown to be important for efficient IgG-mediated

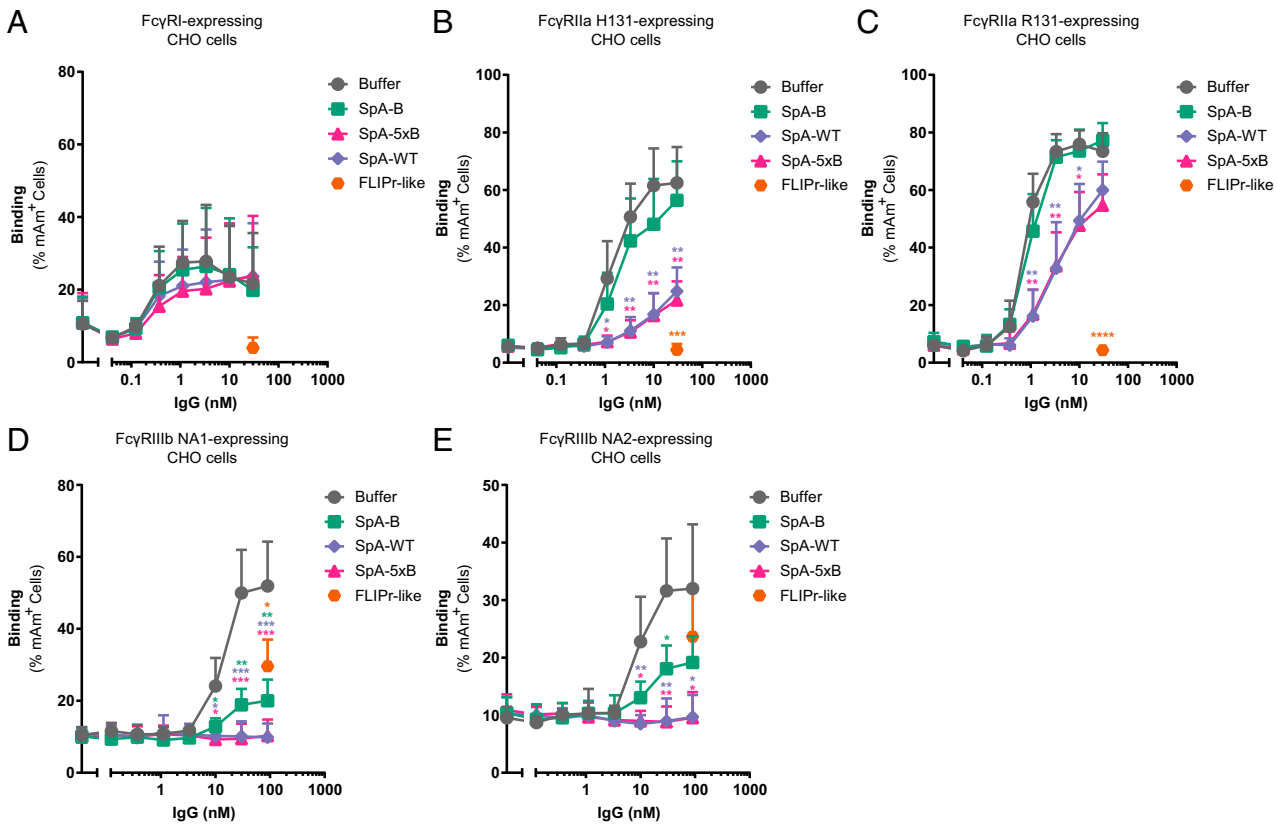

FIGURE 4. Soluble multidomain SpA inhibits binding of FcγRIIa and FcγRIIIb to target-bound IgG1. Binding of anti-WTA IgG1-labeled *S. aureus* Newman Δ*spa/sbi* to hFcγRI- (**A**), hFcγRIIa H131- (**B**), hFcγRIIa R131- (**C**), hFcγRIIIb NA1- (**D**), and hFcγRIIIb NA2-expressing CHO cells (**E**) in absence (buffer; gray) or presence of 200 nM of SpA-B (green), SpA-WT (blue), SpA-5xB (pink), or FLIPr-like (orange), detected by flow cytometry. Bacteria were washed after incubation with IgG1 to remove unbound Abs and only after buffer, SpA, or FLIPr-like was added. Data are presented as percentage of mAm^+ CHO cells ± SD of at least three independent experiments. Statistical analysis was performed using one-way ANOVA to compare buffer condition with SpA-B, SpA-WT, SpA-5xB, and FLIPr-like conditions and displayed only when significant as $*p \leq 0.05$, $**p \leq 0.01$, $***p \leq 0.001$.

phagocytosis of pneumococci (2). We previously suggested that, upon binding of target-bound IgG to FcγRs on the surface of neutrophils, FcRn is translocated to nascent phagosomes, where the low pH promotes binding of FcRn to IgG and facilitates internalization of IgG-opsonized targets (2); additionally, it seems to further promote inflammation in autoimmunity (46). Because SpA and FcRn have an overlapping binding site on the IgG Fc-region (Fig. 1B) and that an analog of the B domain of SpA (the Z domain) was shown to inhibit the binding of FcRn to soluble IgG (47), we also measured the impact of SpA on IgG-FcRn interactions.

We performed flow cytometry experiments in which bacterium-bound IgG1 alone or in combination with each of the SpA constructs, or FLIPr-like, were incubated with FcRn-coated beads at a pH of 6. As expected, all SpA variants reduced IgG1-FcRn interactions, although multidomain SpA proteins were more effective than SpA-B (Fig. 5A, 5B).

We also tested whether there was a difference on the effect of SpA on IgG-FcRn binding when IgGs were in solution. We measured binding of soluble IgG1 to FcRn-coated beads in presence or absence of SpA and showed that all SpA variants reduced IgG1-FcRn interactions, although the single domain was less effective than multidomain SpA proteins (Fig. 5C, 5D). Flow cytometry measurements were corroborated by SPR experiments in which biotinylated FcRn was coupled to streptavidin sensors, and soluble IgG1 alone or in combination with each of the SpA proteins was subsequently injected (Fig. 5E). These data indicate that SpA directly competes with FcRn for binding IgG, and these results may help to clarify how SpA blocks IgG-mediated phagocytosis.

Soluble and surface-bound SpA affect phagocytosis of S. aureus *mediated by naturally occurring Abs*

Finally, we studied the effect of SpA on IgG-mediated phagocytosis in NHS, which contains naturally occurring Abs against *S. aureus*. The serum was HI-NHS to prevent complement activation. Although multidomain SpA proteins were more effective than SpA-B, all SpA constructs reduced Ab-mediated phagocytosis (Fig. 6A, 6B), even though HI-NHS comprises many different Abs, including Abs that bind SpA at different regions (Fc and/or Fab domains) and also Abs that do not bind SpA (as IgG3 and IgM from the non–VH3-type family). We also assessed the impact of cell-surface SpA in reducing phagocytosis in presence of HI-NHS. The efficiency of phagocytosis was reduced when neutrophils were challenged to engulf cell-surface SpA-expressing strains, when compared with Newman Δ*spa*/*sbi,* in particular when the SpA-overexpressing Newman Δ*spa*/*sba* + p*spa*

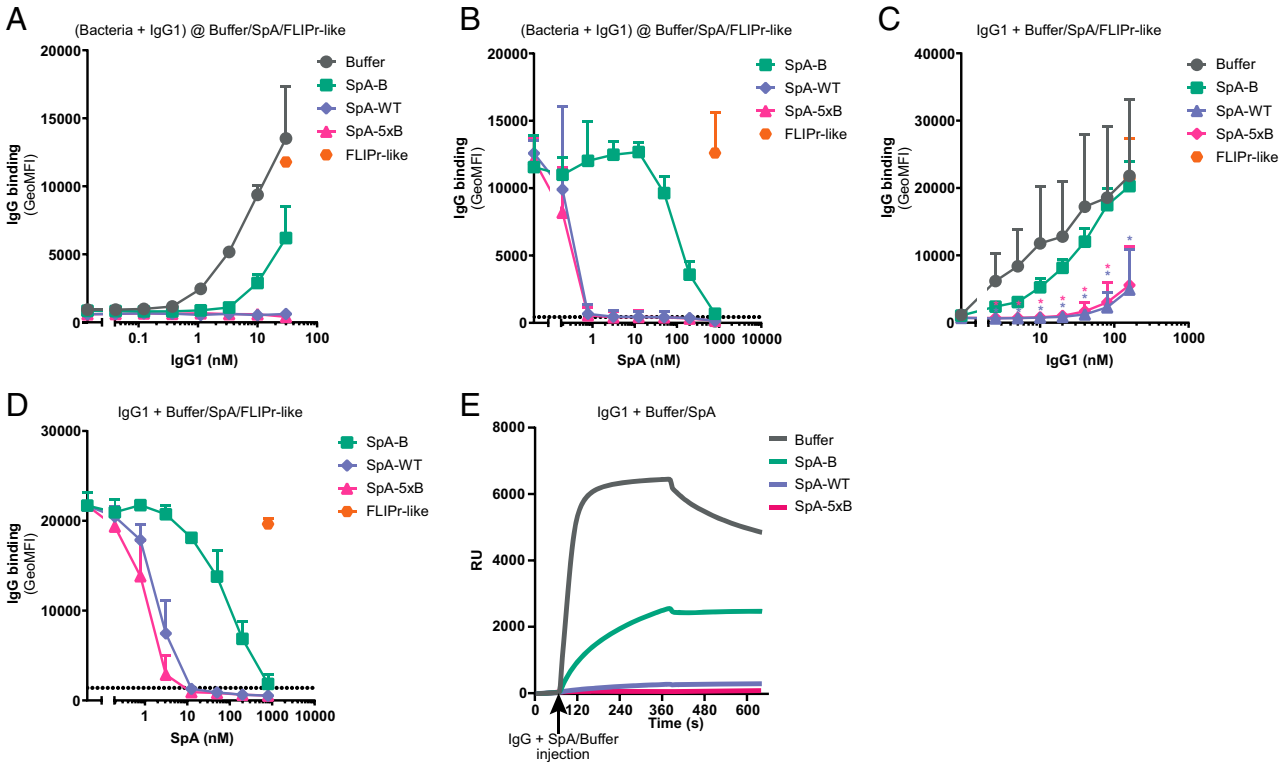

FIGURE 5. Soluble SpA inhibits binding of FcRn to target-bound and soluble IgG1. (**A**) Binding of anti-WTA IgG1-labeled *S. aureus* Newman Δ*spa*/*sbi* to FcRn-coated beads (at pH 6) in absence (buffer; gray) or presence of 200 nM of SpA-B (green), SpA-WT (blue), or SpA-5xB (pink), detected with Alexa Fluor 647–conjugated goat F(ab′)$_2$ anti-human κ by flow cytometry. (**B**) Binding of anti-WTA IgG1-labeled *S. aureus* Newman Δ*spa*/*sbi* bound to FcRn-coated beads in presence of a concentration range of SpA-B (green), SpA-WT (blue), or SpA-5xB (pink), using 10 nM IgG1, detected with Alexa Fluor 647–conjugated goat F(ab′)$_2$ anti-human κ by flow cytometry. The black dotted line shows the background fluorescence from FcRn-coated beads that were incubated with bacteria alone (no IgG). (**C**) Binding of a concentration range of IgG1 to FcRn-coated beads in absence (buffer; gray) or presence of 200 nM SpA-B (green), SpA-WT (blue), SpA-5xB (pink), or FLIPr-like (orange), detected with Alexa Fluor 647–conjugated goat F(ab′)$_2$ anti-human κ by flow cytometry. Statistical analysis was performed using one-way ANOVA to compare buffer condition with SpA-B, SpA-WT, SpA-5xB, and FLIPr-like conditions and displayed only when significant as $*p \leq 0.05$. (**D**) Binding of 10 nM of IgG1 to FcRn-coated beads in presence of a concentration range of SpA-B (green), SpA-WT (blue), SpA-5xB (pink), or FLIPr-like (orange), detected with Alexa Fluor 647–conjugated goat F(ab′)$_2$ anti-human κ by flow cytometry. The black dotted line shows the background fluorescence from the FcRn-coated beads that were not incubated with IgG. (**E**) Sensorgram of SPR measurement for binding of 200 nM of IgG1 to FcRn in absence (buffer; gray) or presence of 1 μM of SpA-B (green), SpA-WT (blue), or SpA-5xB (pink). FcRn was first spotted on the sensor and after IgG1 alone or in combination with SpA-B, SpA-WT, or SpA-5xB was injected at pH 6. Data are presented as mean ± SD of two (A, B, and D) or three (C) independent experiments or as response units (RU) of a single representative experiment (E).

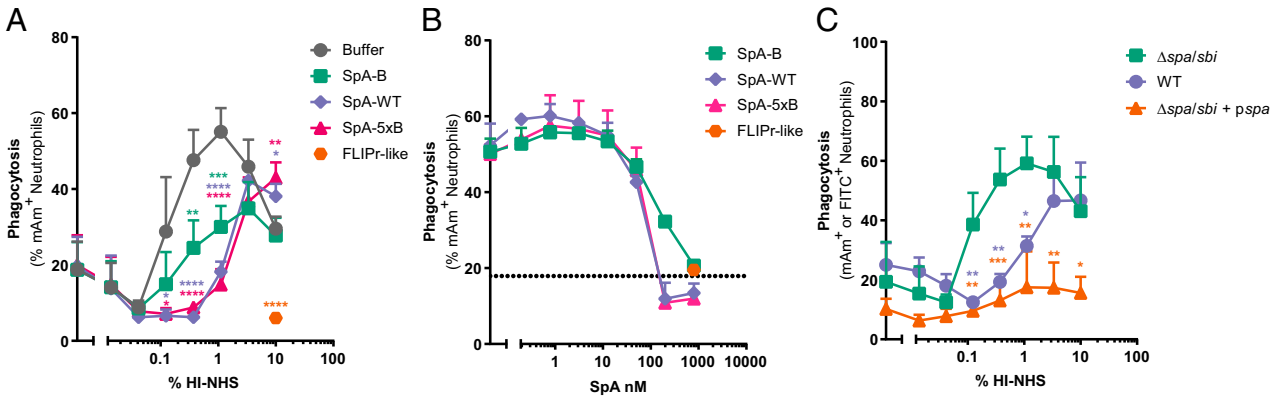

FIGURE 6. Soluble SpA blocks phagocytosis of *S. aureus* mediated by naturally occurring Abs. (**A**) Phagocytosis of *S. aureus* Newman Δ*spa*/*sbi* after incubation of bacteria with a concentration range of HI-NHS, in absence (buffer; gray) or presence of 200 nM soluble SpA-B (green), SpA-WT (blue), SpA-5xB (pink), or FLIPr-like (orange), measured by flow cytometry. Bacteria, IgG, and buffer/SpA were incubated at the same step. Statistical analysis was performed using one-way ANOVA to compare buffer condition with SpA-B, SpA-WT, SpA-5xB, and FLIPr-like conditions and displayed only when significant as $*p \leq 0.05$, $**p \leq 0.01$, $***p \leq 0.001$, $****p \leq 0.0001$. (**B**) Phagocytosis of *S. aureus* Newman Δ*spa*/*sbi* after incubation of bacteria with 1% HI-NHS in presence of a concentration range of SpA-B (green), SpA-WT (blue), or SpA-5xB (pink), measured by flow cytometry. Bacteria, IgG, and buffer/SpA were incubated at the same step. The black dotted line shows the background fluorescence from neutrophils that were incubated with bacteria alone (no IgG). (**C**) Phagocytosis of *S. aureus* Newman Δ*spa*/*sbi*, Newman WT, and Newman Δ*spa*/*sbi* + p*spa* strains after incubation of bacteria with a concentration range of HI-NHS, measured by flow cytometry. Statistical analysis was performed using one-way ANOVA to compare Newman Δ*spa*/*sbi* conditions with Newman WT and Newman Δ*spa*/*sbi* + p*spa* conditions and displayed only when significant as $*p \leq 0.05$, $**p \leq 0.01$, $***p \leq 0.001$. Data are presented as percentage of mAm^+ neutrophils or $FITC^+$ neutrophils ± SD of three (A and C) or two (B) independent experiments.

strain was used that resisted IgG-mediated phagocytosis (Fig. 6C). Altogether, these data show that SpA can block phagocytosis mediated by naturally occurring Abs and that the single SpA-B domain is sufficient to affect it.

Discussion

Abs can help to resolve infections by inducing Fc-effector functions after binding to bacterial surfaces (1). The Fc domains of IgG-labeled bacteria are recognized by FcγRs that are expressed on the surface of innate immune cells (e.g., neutrophils), which engulf and kill bacteria intracellularly. Next to extracellular FcγRs, neutrophils also express FcRn intracellularly, which was shown to facilitate IgG-mediated phagocytosis (2). In this study, we made two important discoveries that may help to understand how SpA from *S. aureus* blocks IgG-mediated phagocytosis: first, we revealed that SpA interferes with the binding of IgG to FcγRIIa and FcγRIIIb; and second, we found that SpA blocks the interaction between IgG and FcRn. Our findings contribute for a better understanding of the immune-evasion mechanisms of *S. aureus*.

This work confirms that both soluble and cell-attached SpA efficiently block FcR-mediated phagocytosis of *S. aureus* by human neutrophils, and, more importantly, it shows that SpA blocks the binding of FcγRIIa, FcγRIIIb, and FcRn to target-bound IgGs. Although SpA has been known to block phagocytosis for a long time (24), the molecular mechanism behind it was not clarified. Although SpA was shown to block binding of IgG-labeled surfaces to Fc receptor–expressing cells (24, 26, 48), soluble murine FcγRI and hFcγRIIa were demonstrated not to compete with SpA for binding to IgG (27). In this study, we confirm that SpA does not affect the binding of the high-affinity hFcγRI to IgG1. However, we show that SpA decreases the binding of IgG1 to the low-affinity receptors FcγRIIa and FcγRIIIb. These conflicting results might be explained by the fact that, instead of soluble FcγRs, we use surface-bound FcγRs, as they better resemble membrane FcγRs. Soluble FcγRs are likely less constrained in their mobility, which may facilitate their binding to SpA-bound IgG molecules.

It has been presumed that SpA, by binding Abs, would simply sequester their Fc sites and, thus, preclude Fc recognition by phagocytic cells (24, 48, 49). Our data suggest that the binding of SpA to IgG1 likely causes a suboptimal steric conformation that affects the binding of low-affinity FcγRs but not high-affinity FcγRs. Importantly, we show that SpA also prevents FcRn from binding IgG. Contrarily to FcγRs that bind IgG-Fc in a structurally distant site from the SpA binding site, FcRn interacts with IgG at the exact same site as SpA. Thus, whereas SpA-IgG interactions likely prevent binding of FcγRs due to steric hindrance, FcRn should compete directly with SpA for binding IgG. Importantly, by blocking binding of FcRn to IgG, SpA may also interfere with other important functions of FcRn. In addition to its role in IgG phagocytosis by neutrophils (2), FcRn also mediates the transfer of IgG from the mother to her fetus (50) and extends the serum half-life of IgG (5, 51). More recently, FcRn was also found to regulate Ag presentation (52), Ag cross-presentation (53, 54), and secretion of cytotoxicity-promoting cytokines by dendritic cells (53). Therefore, we expect that SpA has a much broader immunomodulatory action than initially anticipated.

This study also provides a rationale for the multiplicity of repeating Ig-binding domains of SpA produced by *S. aureus*. In fact, we show that SpA needs to be composed of multiple Ig-binding domains to efficiently block IgG1-mediated phagocytosis and to decrease the binding of IgG1 to FcγRIIa-coated surfaces. It is possible that a multidomain SpA molecule that is bound to IgG1-opsonized bacteria can still bind to soluble IgGs, forming IgG-SpA complexes that make IgG–Fc tails inaccessible to FcγRs. However, experiments where the bacteria were first incubated with IgGs and then washed suggest that SpA binds to bacterium-bound IgGs to block IgG-FcγR interactions and, consequently, phagocytosis. Thus, a more plausible hypothesis is that SpA needs multiple IgG-binding domains to cause steric hindrance and mask the FcγR binding site on IgG1-opsonized bacteria. This hypothesis is supported by the fact that SpA composed of five domains binds IgG with a 1:1 stoichiometry (22), which suggests that two of the five domains of SpA bind to both sites of IgG-Fc, leaving the other three domains free to cover the region in

IgG where FcγRs bind. However, this theory does not explain why the single SpA-B domain affects IgG–FcγRIIIb binding. We speculate that this is a consequence of a slight change to the CH2 configuration of the IgG that is induced by the binding of SpA-B, which has a particularly strong impact (relative) on the lowest-affinity FcγR.

Although further studies are needed to clarify how SpA-B affects IgG2- and IgG4-mediated phagocytosis and whether the target of the Ab influences FcγR and/or FcRn recognition, we suggest that SpA-B may be used as a research tool to assess which FcRs drive IgG-mediated phagocytosis. Because the effect of SpA-B on phagocytosis mediated by anti-WTA IgG1 was very minor, it is likely that this Ab mediates phagocytosis mainly by triggering FcγRIIa. Conversely, because the single SpA-B domain was sufficient to effectively reduce phagocytosis mediated by naturally occurring Abs, FcRn and/or FcγRIIIb may play a more essential role in the phagocytosis mediated by other Ab types.

Around 85% of SpA produced by *S. aureus* is anchored to the cell wall of the bacteria (14). We envision that cell-attached SpA might inhibit IgG-mediated phagocytosis of *S. aureus* by the same mechanisms described in this study for soluble SpA. However, we also speculate that cell-attached SpA could induce an additional inhibitory mechanism by covering the *S. aureus* surface with Abs, creating a shield that prevents anti–*S. aureus* Abs from reaching the bacterial surface and/or that masks their binding sites, as suggested before (24). Another hypothesis is that their binding sites are already occupied by Abs that simultaneously bind to cell-surface SpA (via the Fc domain) and to their target Ag on the bacterial surface (via Fab domain), the so-called phenomenon "bipolar bridging."

Our study also provides a rational for the design of therapeutic Abs against staphylococcal infections. Although all IgG1 allotypes harbor a His at the 435 position, only 5 of the 29 reported allelic variants of IgG3 are H435-containing allotypes and, thus, SpA binders (18, 19). In line with our previous study (22), we show in this study that a R435-containing IgG3 allotype is unaffected by the presence of SpA and thus is more potent to mediate phagocytosis and killing of *S. aureus* by neutrophils than IgG1. Therefore, we suggest that mAbs against the *S. aureus* surface should be developed as R435-containing allotypes of IgG3 Abs. The fact that IgG3 Abs are the most effective IgG subclass to trigger immune effector functions (55) also supports this selection.

In conclusion, this study contributes for our understanding of how SpA blocks IgG-mediated phagocytosis of *S. aureus* and may also help the development of therapeutic options to tackle staphylococcal infections.

Acknowledgments

We thank Dr. Annette M. Stemerding for fruitful discussions.

Disclosures

A.R.C. participated in a postgraduate studentship program at GlaxoSmithKline. K.P.M.v.K. and S.H.M.R. are co-inventors on a patent describing Ab therapies against *S. aureus*. The other authors have no financial conflicts of interest.

References

1. Lu, L. L., T. J. Suscovich, S. M. Fortune, and G. Alter. 2018. Beyond binding: antibody effector functions in infectious diseases. *Nat. Rev. Immunol.* 18: 46–61.
2. Vidarsson, G., A. M. Stemerding, N. M. Stapleton, S. E. Spliethoff, H. Janssen, F. E. Rebers, M. de Haas, and J. G. van de Winkel. 2006. FcRn: an IgG receptor on phagocytes with a novel role in phagocytosis. *Blood* 108: 3573–3579.
3. Story, C. M., J. E. Mikulska, and N. E. Simister. 1994. A major histocompatibility complex class I-like Fc receptor cloned from human placenta: possible role in transfer of immunoglobulin G from mother to fetus. *J. Exp. Med.* 180: 2377–2381.
4. Israel, E. J., D. F. Wilsker, K. C. Hayes, D. Schoenfeld, and N. E. Simister. 1996. Increased clearance of IgG in mice that lack β 2-microglobulin: possible protective role of FcRn. *Immunology* 89: 573–578.
5. Ghetie, V., J. G. Hubbard, J. K. Kim, M. F. Tsen, Y. Lee, and E. S. Ward. 1996. Abnormally short serum half-lives of IgG in β 2-microglobulin-deficient mice. *Eur. J. Immunol.* 26: 690–696.
6. Zhu, X., G. Meng, B. L. Dickinson, X. Li, E. Mizoguchi, L. Miao, Y. Wang, C. Robert, B. Wu, P. D. Smith, et al. 2001. MHC class I-related neonatal Fc receptor for IgG is functionally expressed in monocytes, intestinal macrophages, and dendritic cells. *J. Immunol.* 166: 3266–3276.
7. Caaveiro, J. M. M., M. Kiyoshi, and K. Tsumoto. 2015. Structural analysis of Fc/FcγR complexes: a blueprint for antibody design. *Immunol. Rev.* 268: 201–221.
8. Sánchez, L. M., D. M. Penny, and P. J. Bjorkman. 1999. Stoichiometry of the interaction between the major histocompatibility complex-related Fc receptor and its Fc ligand. *Biochemistry* 38: 9471–9476.
9. Abdiche, Y. N., Y. A. Yeung, J. Chaparro-Riggers, I. Barman, P. Strop, S. M. Chin, A. Pham, G. Bolton, D. McDonough, K. Lindquist, et al. 2015. The neonatal Fc receptor (FcRn) binds independently to both sites of the IgG homodimer with identical affinity. *MAbs* 7: 331–343.
10. West, A. P., Jr., and P. J. Bjorkman. 2000. Crystal structure and immunoglobulin G binding properties of the human major histocompatibility complex-related Fc receptor(,). *Biochemistry* 39: 9698–9708.
11. Rodewald, R. 1976. pH-dependent binding of immunoglobulins to intestinal cells of the neonatal rat. *J. Cell Biol.* 71: 666–669.
12. Sidorin, E. V., and T. F. Solov'eva. 2011. IgG-binding proteins of bacteria. *Biochemistry (Mosc.)* 76: 295–308.
13. Lowy, F. D. 1998. *Staphylococcus aureus* infections. *N. Engl. J. Med.* 339: 520–532.
14. Becker, S., M. B. Frankel, O. Schneewind, and D. Missiakas. 2014. Release of protein A from the cell wall of *Staphylococcus aureus*. *Proc. Natl. Acad. Sci. USA* 111: 1574–1579.
15. O'Halloran, D. P., K. Wynne, and J. A. Geoghegan. 2015. Protein A is released into the *Staphylococcus aureus* culture supernatant with an unprocessed sorting signal. *Infect. Immun.* 83: 1598–1609.
16. Deisenhofer, J. 1981. Crystallographic refinement and atomic models of a human Fc fragment and its complex with fragment B of protein A from *Staphylococcus aureus* at 2.9- and 2.8-A resolution. *Biochemistry* 20: 2361–2370.
17. Graille, M., E. A. Stura, A. L. Corper, B. J. Sutton, M. J. Taussig, J. B. Charbonnier, and G. J. Silverman. 2000. Crystal structure of a *Staphylococcus aureus* protein A domain complexed with the Fab fragment of a human IgM antibody: structural basis for recognition of B-cell receptors and superantigen activity. *Proc. Natl. Acad. Sci. USA* 97: 5399–5404.
18. Van Loghem, E., B. Frangione, B. Recht, and E. C. Franklin. 1982. Staphylococcal protein A and human IgG subclasses and allotypes. *Scand. J. Immunol.* 15: 275–278.
19. Chu, T. H., E. F. Patz, Jr., and M. E. Ackerman. 2021. Coming together at the hinges: therapeutic prospects of IgG3. *MAbs* 13: 1882028.
20. Jendeberg, L., P. Nilsson, A. Larsson, P. Denker, M. Uhlén, B. Nilsson, and P. Å. Nygren. 1997. Engineering of Fc(1) and Fc(3) from human immunoglobulin G to analyse subclass specificity for staphylococcal protein A. *J. Immunol. Methods* 201: 25–34.
21. de Taeye, S. W., A. E. H. Bentlage, M. M. Mebius, J. I. Meesters, S. Lissenberg-Thunnissen, D. Falck, T. Sénard, N. Salehi, M. Wuhrer, J. Schuurman, et al. 2020. FcγR binding and ADCC activity of human IgG allotypes. *Front. Immunol.* 11: 740.
22. Cruz, A. R., M. A. D. Boer, J. Strasser, S. A. Zwarthoff, F. J. Beurskens, C. J. C. de Haas, P. C. Aerts, G. Wang, R. N. de Jong, F. Bagnoli, et al. 2021. Staphylococcal protein A inhibits complement activation by interfering with IgG hexamer formation. *Proc. Natl. Acad. Sci. USA* 118: e2016772118.
23. Falugi, F., H. K. Kim, D. M. Missiakas, and O. Schneewind. 2013. Role of protein A in the evasion of host adaptive immune responses by *Staphylococcus aureus*. *mBio* 4: e00575-13.
24. Dossett, J. H., G. Kronvall, R. C. Williams, Jr., and P. G. Quie. 1969. Antiphagocytic effects of staphylococcal protein A. *J. Immunol.* 103: 1405–1410.
25. Diebolder, C. A., F. J. Beurskens, R. N. de Jong, R. I. Koning, K. Strumane, M. A. Lindorfer, M. Voorhorst, D. Ugurlar, S. Rosati, A. J. R. Heck, et al. 2014. Complement is activated by IgG hexamers assembled at the cell surface. *Science* 343: 1260–1263.
26. Sulica, A., C. Medesan, M. Laky, D. Onică, J. Sjöquist, and V. Ghetie. 1979. Effect of protein A of *Staphylococcus aureus* on the binding of monomeric and polymeric IgG to Fc receptor-bearing cells. *Immunology* 38: 173–179.
27. Wines, B. D., M. S. Powell, P. W. H. I. Parren, N. Barnes, and P. M. Hogarth. 2000. The IgG Fc contains distinct Fc receptor (FcR) binding sites: the leukocyte receptors Fc γ RI and Fc γ RIIa bind to a region in the Fc distinct from that recognized by neonatal FcR and protein A. *J. Immunol.* 164: 5313–5318.
28. Gonzalez, M. L., M. B. Frank, P. A. Ramsland, J. S. Hanas, and F. J. Waxman. 2003. Structural analysis of IgG2A monoclonal antibodies in relation to complement deposition and renal immune complex deposition. *Mol. Immunol.* 40: 307–317.
29. Lehar, S. M., T. Pillow, M. Xu, L. Staben, K. K. Kajihara, R. Vandlen, L. DePalatis, H. Raab, W. L. Hazenbos, J. H. Morisaki, et al. 2015. Novel antibody-antibiotic conjugate eliminates intracellular *S. aureus*. *Nature* 527: 323–328.
30. Ling, W. L., W. H. Lua, J. J. Poh, J. Y. Yeo, D. P. Lane, and S. K. E. Gan. 2018. Effect of VH-VL families in pertuzumab and trastuzumab recombinant production, Her2 and FcγIIA binding. *Front. Immunol.* 9: 469.

31. Vink, T., M. Oudshoorn-Dickmann, M. Roza, J. J. Reitsma, and R. N. de Jong. 2014. A simple, robust and highly efficient transient expression system for producing antibodies. *Methods* 65: 5–10.
32. Prat, C., P.-J. Haas, J. Bestebroer, C. J. C. de Haas, J. A. G. van Strijp, and K. P. M. van Kessel. 2009. A homolog of formyl peptide receptor-like 1 (FPRL1) inhibitor from *Staphylococcus aureus* (FPRL1 inhibitory protein) that inhibits FPRL1 and FPR. *J. Immunol.* 183: 6569–6578.
33. Boero, E., I. Brinkman, T. Juliet, E. van Yperen, J. A. G. van Strijp, S. H. M. Rooijakkers, and K. P. M. van Kessel. 2021. Use of flow cytometry to evaluate phagocytosis of *Staphylococcus aureus* by human neutrophils. *Front. Immunol.* 12: 635825.
34. de Jong, N. W. M., T. van der Horst, J. A. G. van Strijp, and R. Nijland. 2017. Fluorescent reporters for markerless genomic integration in *Staphylococcus aureus. Sci. Rep.* 7: 43889.
35. Pang, Y. Y., J. Schwartz, M. Thoendel, L. W. Ackermann, A. R. Horswill, and W. M. Nauseef. 2010. agr-Dependent interactions of *Staphylococcus aureus* USA300 with human polymorphonuclear neutrophils. *J. Innate Immun.* 2: 546–559.
36. Surewaard, B. G. J., J. A. G. van Strijp, and R. Nijland. 2013. Studying interactions of *Staphylococcus aureus* with neutrophils by flow cytometry and time lapse microscopy. *J. Vis. Exp.* 77: e50788.
37. Dekkers, G., A. E. H. Bentlage, T. C. Stegmann, H. L. Howie, S. Lissenberg-Thunnissen, J. Zimring, T. Rispens, and G. Vidarsson. 2017. Affinity of human IgG subclasses to mouse Fc gamma receptors. *MAbs* 9: 767–773.
38. Lux, A., X. Yu, C. N. Scanlan, and F. Nimmerjahn. 2013. Impact of immune complex size and glycosylation on IgG binding to human FcγRs. *J. Immunol.* 190: 4315–4323.
39. Zhang, L., K. Jacobsson, J. Vasi, M. Lindberg, and L. Frykberg. 1998. A second IgG-binding protein in *Staphylococcus aureus. Microbiology (Reading)* 144: 985–991.
40. Brown, S., J. P. Santa Maria, Jr., and S. Walker. 2013. Wall teichoic acids of gram-positive bacteria. *Annu. Rev. Microbiol.* 67: 313–336.
41. Stemerding, A. M., J. Köhl, M. K. Pandey, A. Kuipers, J. H. Leusen, P. Boross, M. Nederend, G. Vidarsson, A. Y. L. Weersink, J. G. J. van de Winkel, et al. 2013. *Staphylococcus aureus* formyl peptide receptor-like 1 inhibitor (FLIPr) and its homologue FLIPr-like are potent FcγR antagonists that inhibit IgG-mediated effector functions. *J. Immunol.* 191: 353–362.
42. Fong, R., K. Kajihara, M. Chen, I. Hotzel, S. Mariathasan, W. L. W. Hazenbos, and P. J. Lupardus. 2018. Structural investigation of human *S. aureus*-targeting antibodies that bind wall teichoic acid. *MAbs* 10: 979–991.
43. Nathan, C. 2006. Neutrophils and immunity: challenges and opportunities. *Nat. Rev. Immunol.* 6: 173–182.
44. Wang, Y., and F. Jönsson. 2019. Expression, role, and regulation of neutrophil Fcγ receptors. *Front. Immunol.* 10: 1958.
45. Kerntke, C., F. Nimmerjahn, and M. Biburger. 2020. There is (scientific) strength in numbers: a comprehensive quantitation of Fc gamma receptor numbers on human and murine peripheral blood leukocytes. *Front. Immunol.* 11: 118.
46. Hubbard, J. J., M. Pyzik, T. Rath, L. K. Kozicky, K. M. K. Sand, A. K. Gandhi, A. Grevys, S. Foss, S. C. Menzies, J. N. Glickman, et al. 2020. FcRn is a CD32a coreceptor that determines susceptibility to IgG immune complex-driven autoimmunity. *J. Exp. Med.* 217: e20200359.
47. Raghavan, M., M. Y. Chen, L. N. Gastinel, and P. J. Bjorkman. 1994. Investigation of the interaction between the class I MHC-related Fc receptor and its immunoglobulin G ligand. *Immunity* 1: 303–315.
48. Rosenblatt, J., P. M. Zeltzer, J. Portaro, and R. C. Seeger. 1977. Inhibition of antibody-dependent cellular cytotoxicity by protein A from *Staphylococcus aureus. J. Immunol.* 118: 981–985.
49. Kobayashi, S. D., and F. R. DeLeo. 2013. *Staphylococcus aureus* protein A promotes immune suppression. *mBio* 4: e00764-13.
50. Simister, N. E., and K. E. Mostov. 1989. An Fc receptor structurally related to MHC class I antigens. *Nature* 337: 184–187.
51. Junghans, R. P., and C. L. Anderson. 1996. The protection receptor for IgG catabolism is the β2-microglobulin-containing neonatal intestinal transport receptor. *Proc. Natl. Acad. Sci. USA* 93: 5512–5516.
52. Qiao, S. W., K. Kobayashi, F. E. Johansen, L. M. Sollid, J. T. Andersen, E. Milford, D. C. Roopenian, W. I. Lencer, and R. S. Blumberg. 2008. Dependence of antibody-mediated presentation of antigen on FcRn. *Proc. Natl. Acad. Sci. USA* 105: 9337–9342.
53. Baker, K., T. Rath, M. B. Flak, J. C. Arthur, Z. Chen, J. N. Glickman, I. Zlobec, E. Karamitopoulou, M. D. Stachler, R. D. Odze, et al. 2013. Neonatal Fc receptor expression in dendritic cells mediates protective immunity against colorectal cancer. *Immunity* 39: 1095–1107.
54. Baker, K., S. W. Qiao, T. T. Kuo, V. G. Aveson, B. Platzer, J. T. Andersen, I. Sandlie, Z. Chen, C. de Haar, W. I. Lencer, et al. 2011. Neonatal Fc receptor for IgG (FcRn) regulates cross-presentation of IgG immune complexes by CD8-CD11b+ dendritic cells. *Proc. Natl. Acad. Sci. USA* 108: 9927–9932.
55. Vidarsson, G., G. Dekkers, and T. Rispens. 2014. IgG subclasses and allotypes: from structure to effector functions. *Front. Immunol.* 5: 520.